Localized Traveling-Wave States in Binary-Fluid Convection

Joseph J. Niemela, Guenter Ahlers, and David S. Cannell
Department of Physics and Center for Nonlinear Science, University of California, Santa Barbara, California 93106
(Received 7 November 1989)

We report on convection in horizontal layers of an ethanol-water mixture in a rectangular and an annular container heated from below. When the temperature difference ΔT exceeds a critical value, localized regions of traveling-wave convection evolve via a backward bifurcation in both geometries and coexist with the conduction state for a *range* of ΔT. The size, shape, wave number, and frequency of the localized states are reproducible and geometry independent. The coexistence *range* stands in contrast to systems with a potential, where droplets of a given phase are not stable for first-order transitions at fixed values of the thermodynamic fields.

PACS numbers: 47.20.Bp, 47.25.−c

Convection in binary-fluid mixtures has attracted considerable theoretical[1-5] and experimental[6-12] interest recently. This is largely because the transition from conduction to convection yields a time-periodic state which consists of traveling waves (TW), i.e., of convection rolls which move in a direction perpendicular to their axes. Particularly intriguing has been the observation that a backward bifurcation, analogous to a first-order phase transition in thermodynamic systems, can lead to localized traveling waves (LTW) which coexist with regions of pure conduction for a range of temperature differences ΔT.[8,9] A coexistence *range* for the two phases stands in contrast to thermodynamic systems, where the existence of an extremum principle assures that two phases coexist in steady state only for a unique temperature when the other thermodynamic fields are held constant.

It has been suggested that the observed coexistence *range* of LTW and conduction can be explained by the interaction of the TW with the short sidewalls of the rectangular containers of the experiments.[1,2,9-12] Indeed, numerical calculations based on two coupled Ginzburg-Landau (GL) equations and reflection of the TW from the wall towards which they are traveling were able to reproduce some features of the early experiments.[1,2] We report in this Letter quantitative measurements of the size, shape, wave number, frequency, and convective heat transport of LTW in both rectangular and annular containers. We find that the localized states have essentially identical properties in the two geometries. Since the annulus has no sidewalls parallel to the roll axis, reflection cannot be invoked as a stabilizing mechanism.

Our observations agree qualitatively with theoretical work by Thual and Fauve.[5] These authors initially studied a single GL equation with real coefficients. In common with thermodynamic systems, this equation has a potential which is a minimum for the steady state. From it they were unable to produce stable LTW states. However, with complex coefficients (appropriate for describing binary-fluid convection) this equation has no potential. In that case, Thual and Fauve found a coexistence range for LTW and conduction. Their localized states have unique spatial extents and wave vectors which decrease from the trailing to the leading edge, in common with our experimental observations. However, the envelopes of their LTW move with a characteristic speed in the laboratory frame, whereas in our experimental system these envelopes are at rest in steady state.

We used identical mixtures of 25.0% by weight ethanol in water in both a rectangle of height $d=0.363$ cm and height-to-width-to-length ratio 1:2.0:22, and an annulus of height $d=0.354$ cm and height-to-(radial width)-to-(mean circumference) ratio of 1:2.0:63, under otherwise nominally identical conditions. Both cells had Delrin sidewalls which were sealed to the top and bottom plates with O rings. Otherwise the apparatus and procedure were similar to those described elsewhere.[13] Shadowgraph flow-visualization and heat-flux measurements could be made. The top plates of the cells were maintained at 26.0 °C. The critical temperature difference was $\Delta T_c \cong 1.53$ °C (1.62 °C) for the rectangle (annulus). We estimate a mean separation ratio[14] $\psi \simeq -0.08$, a Lewis number of 0.01, and a Prandtl number of 19. The convective threshold was found by incrementing the heat current q applied to the bottom plate in steps of 0.1% through its critical value q_c and waiting for times of approximately $100\tau_v$, where $\tau_v \cong 120$ sec is the vertical thermal diffusion time d^2/κ with κ the thermal diffusivity. For the critical Rayleigh number R_c we find $R_c^r = 1966$ for the rectangle and $R_c^a = 1933$ for the annulus. The threshold shift $\epsilon_s = R_c^r/R_c^a - 1 = 0.017 \pm 0.003$ is consistent with the stabilization predicted[2] to occur in a finite-length cell because of reflection of traveling waves from the end walls, and with other experimental observations.[10,11] Below we will scale all lengths by d and times by τ_v.

After increasing q above q_c, counterpropagating TW occupied the entire rectangle during the early stages of a transient.[6-8] At intermediate times, this convective flow evolved into confined domains of primarily left-going TW and right-going TW in the left and right halves of the rectangular cell, respectively. During nominally identical experimental runs a LTW state on the left or

© 1990 The American Physical Society

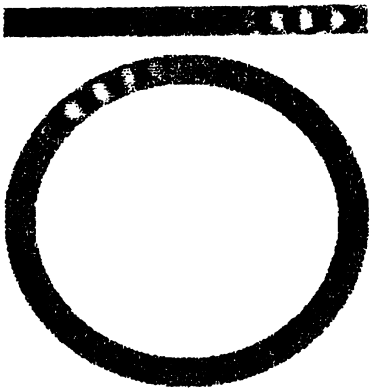

FIG. 1. Shadowgraph images of steady-state convective flow patterns in the rectangle and in the annulus. The TW in the annulus are moving counterclockwise, and those in the rectangle are moving to the right.

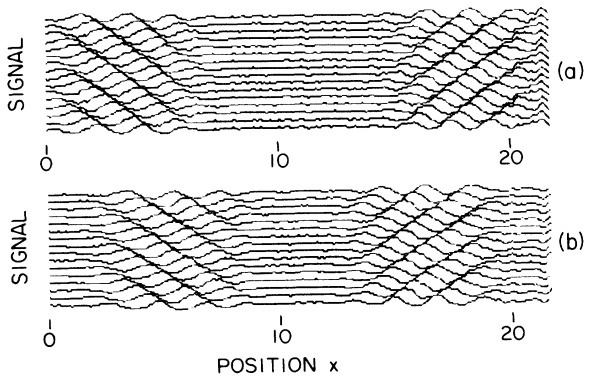

FIG. 2. Space-time contour plots of the shadowgraph signal for a double-LTW state in the rectangle: (a) Near the convective threshold ($\epsilon = -0.004$) and (b) just prior to losing the right-hand LTW near the saddle node ($\epsilon = -0.014$).

on the right, or on both ends, would survive at later times. Its envelope would move in the direction of the TW, and come to rest near the end wall. During the transient the frequency of the TW decreased quickly from $\omega \cong 6$, which is very near the Hopf frequency, to $\omega = 2.70$. The transient evolution in the annulus was similar in the sense that convection began throughout the system when ΔT_c was first exceeded, and at later times evolved to one or more LTW which had sizes, frequencies, and wave vectors similar to the LTW states in the rectangle. Once formed, the LTW states in the annulus initially also moved in the direction of their TW, but eventually they came to rest. Within our resolution, the LTW position approached its equilibrium value exponentially, with a characteristic time of about $200\tau_v$. Typical steady states are shown in Fig. 1.

To make clear the traveling-wave nature of the confined rolls, we show in Fig. 2 space-time contour plots corresponding to a double-LTW steady state in the rectangle. Each contour line is obtained by taking an average of the shadowgraph signal over the central 50% of a particular image for each position along the length of the cell. The lines are spaced $0.56\tau_v$ apart, with time increasing from bottom to top. In Fig. 2(a), the envelopes of both LTW are at rest near their respective sidewalls. While this is a stable state near threshold, the LTW do not always remain against the wall; after decreasing $\epsilon = R/R_c - 1$ below a certain value, the envelopes moved in a direction opposite that of their respective TW, thus approaching each other. The movement after a change in ϵ is a transient, and the envelope came to rest at a new location after some time, as shown in Fig. 2(b) for $\epsilon = -0.014$. This movement, in a direction opposite the confined TW, is a characteristic feature at sufficiently negative ϵ; we also observed it for LTW states in the annulus, and for single LTW states of either left- or right-traveling waves in the rectangle. Making ϵ less negative reversed this process. This movement of the LTW envelopes proves useful, in that it allows us to prepare and analyze states in the rectangle which have negligible interaction with the walls. This is particularly useful when making detailed comparisons between observations in the rectangle and annulus.

One method of comparing convective states in the two geometries is to examine the heat transport in each system. In Fig. 3(a) we show heat-transfer data corre-

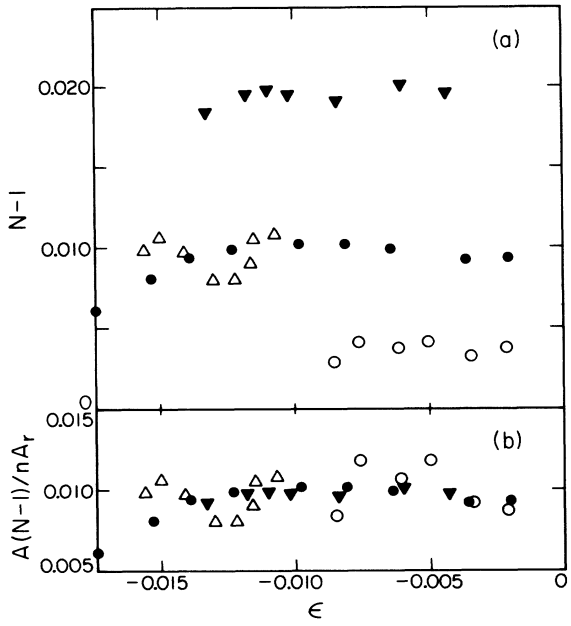

FIG. 3. Heat transfer for a single-LTW state in the annulus (open circles); single-LTW state of right-traveling waves in the rectangle (solid circles); double-LTW state in the rectangle (solid inverted triangles); and single-LTW state of left-traveling waves in the rectangle following loss of the right-traveling state in the two-state case (open triangles). (a) Reduced Nusselt number $N-1$ vs ϵ. (b) Normalized Nusselt number $(N-1)A/nA_r$ for data in (a), where n is the number of LTW states in the cell, A_r is the lateral cross-sectional area of the rectangle, and A is the area of the cell under consideration.

sponding to the runs described above in terms of a reduced Nusselt number $N-1$, where N is defined as the ratio of the effective thermal conductivity of the fluid layer to that due to thermal conduction alone. The difference in Nusselt number for the various runs can be attributed to the different relative areas of the convecting and conducting regions. To demonstrate this, we divided the reduced Nusselt number by a factor nA_r/A, where n corresponds to the number of LTW states present, A_r is the lateral cross-sectional area of fluid contained in the rectangular cell, and A is that area for the cell in question (rectangle or annulus). In Fig. 3(b) we plot the quantity $(N-1)A/nA_r$ as a function of ϵ for the data of Fig. 3(a). It is evident that the heat transported convectively, per LTW state, is essentially the same for all the observed states.

For further comparison between the LTW states in the rectangle and annulus, we fitted a function derived[15] from a fifth-order Ginzburg-Landau equation with complex coefficients to individual contour lines $I(x)$ by a least-squares method. The function describes both the rapid variation of the individual convective rolls and an overall envelope. It is

$$I(x)=I_0F(x)\cos[\theta(x)]+I_B\,, \tag{1a}$$

where I_B is a linearly varying background term which accounts for experimental effects, and $F(x)$ describes an envelope centered about $x=x_0$ given by

$$F^2(x)=\eta\exp[2m(x-x_0)]\{\eta-1+(1-\eta/2+(\eta/2)\exp[2m(x-x_0)])^2\}^{-1}. \tag{1b}$$

Its characteristic width l, defined as the full width at half maximum of $F(x)$, is

$$l=\ln\{1+6/\eta+(2/\eta)[3(3+\eta)]^{1/2}\}/m\,. \tag{1c}$$

The cosine argument

$$\theta(x)=[k_0+k_1K(x)](x-x_0)+\phi\,, \tag{1d}$$

with

$$K(x)=\mathrm{sgn}(x-x_0)m[1-F^2(x)]^{1/2}\times[1+(\eta-1)F^2(x)]^{1/2}, \tag{1e}$$

describes the rapid variation of the convective pattern. We found ϕ to vary linearly with time, with $\dot\phi$ equal to the traveling-wave frequency ω. In Figs. 4(a) and 4(b) we illustrate two examples. An LTW state in the annulus near onset ($\epsilon\cong-0.001$) is shown in Fig. 4(a). Here, the rolls are moving to the right as indicated by the arrow. Similarly, in Fig. 4(b) we show a LTW state, also of right-going TW, from the rectangle at $\epsilon\cong-0.013$, where the center of the LTW, as discussed above, has moved away from the right end wall. The values of the parameters are given in the figure caption.

In Fig. 5 we plot values of l vs ϵ for both the annulus and the rectangle. The error bars represent the standard deviation about the mean value of l obtained from fitting between 30 and 100 consecutive scan lines at each ϵ. The data vary little over the range of ϵ shown. More importantly, there is no significant difference between the two geometries, and $l\cong5.0$ for both systems.

A remarkable property of the LTW states implied by Fig. 5 is their stability for positive ϵ, where the conducting state is unstable. One possible explanation might be stabilizing azimuthal concentration variations induced by the LTW. We ruled this out by cycling the annulus to the conducting state below the saddle node and once more to positive ϵ. Convection began uniformly rather than being localized at the old LTW location as would have been expected. Another possibility is that, under conditions where the conducting state is convectively but

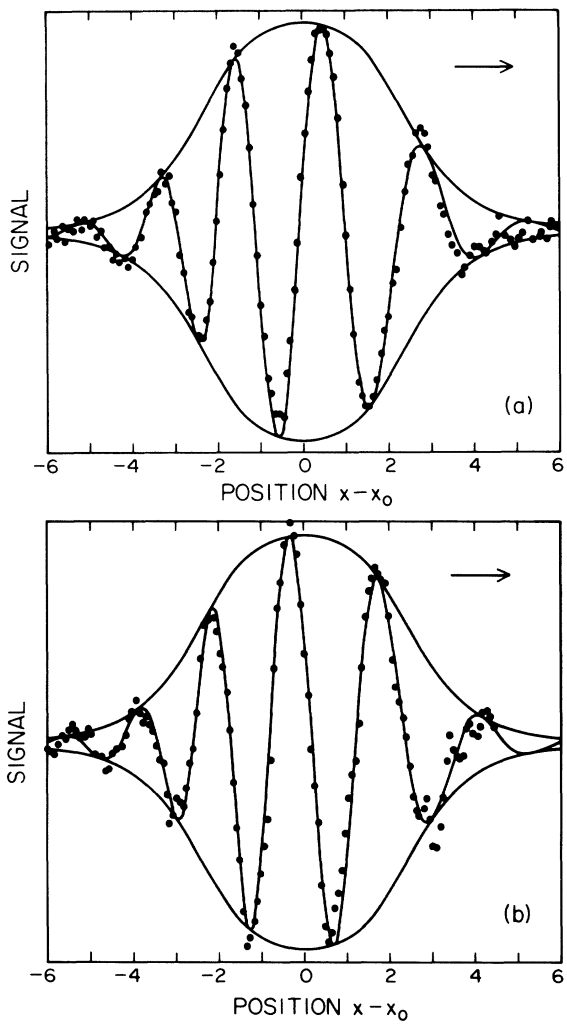

FIG. 4. Fit of Eq. (1) to shadowgraph-intensity data (solid circles) for LTW's. The background I_B has been subtracted. Both $I(x)-I_B$ and the envelope [$I_0F(x)$ and $-I_0F(x)$] are shown as solid lines. (a) Annulus ($\epsilon\cong-0.001$, $m=0.94$, $\eta=0.11$, $k_0=2.99$, $k_1=-0.41$, $l=5.05$). (b) Rectangle ($\epsilon\cong-0.013$, $m=0.93$, $\eta=0.08$, $k_0=3.16$, $k_1=-0.40$, $l=5.16$).

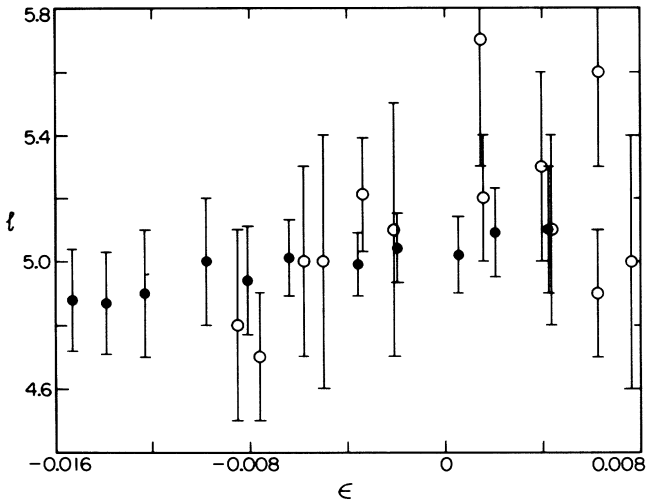

FIG. 5. The width l as a function of ϵ for LTW states in the rectangle (solid circles) and annulus (open circles).

not absolutely unstable, perturbations, which travel as they grow, cannot reach an observable amplitude before encountering the LTW. Since we cannot estimate the amplitude of such fluctuations we cannot predict when this might occur, except that it should be for $\epsilon \leq 0.06$ where we estimate[2,4] the conducting state becomes absolutely unstable. Experimentally, however, we have not observed LTW states to be stable in the annulus for $\epsilon \gtrsim 0.01$.

The TW frequencies of the various localized states are all about half the Hopf frequency, and increase somewhat with decreasing ϵ. The frequency in the annulus rises from about $\omega = 2.50$, for the steady state at onset, to $\omega = 3.04$ at the saddle node. In the rectangle we observed it to increase from $\omega = 2.53$, for a LTW state of left-going rolls at onset, to a maximum of $\omega = 3.09$ at the saddle node. The measured frequencies of the left-TW and right-TW states with two LTW present in the rectangle can differ by as much as 6% at a given value of ϵ. There is a similar difference in the wave number, although the phase velocity ω/k_0 has nearly the same value and increases with decreasing ϵ to a maximum of 1.0 at the saddle node. Likewise, the phase velocity of convection rolls in the annulus attains a maximum value near 1.0 at its saddle node.

It is important to note that the LTW studied by us differ qualitatively from those observed by Kolodner, Bensimon, and Surko[12] for different experimental parameters. Theirs had a spatial extent which depended upon the experimental protocol, whereas the ones discussed here have a unique size.

We wish to thank H. R. Brand, M. C. Cross, P. Kolodner, and W. Schoepf for helpful conversations, W. van Saarloos and P. C. Hohenberg for communicating their theoretical results to us prior to publication, and the IBM Corporation for support for one of us (J.N.). This work was supported by the Department of Energy under Grant No. DOE 84ER 13729.

[1]M. C. Cross, Phys. Rev. Lett. **57**, 2935 (1986).
[2]M. C. Cross, Phys. Rev. A **38**, 3593 (1988).
[3]E. Knobloch, Phys. Rev. A **34**, 1538 (1986), and references therein.
[4]M. C. Cross and K. Kim, Phys. Rev. A **37**, 3909 (1988).
[5]O. Thual and S. Fauve, J. Phys. (Paris) **49**, 1829 (1988).
[6]P. Kolodner, A. Passner, C. M. Surko, and R. W. Walden, Phys. Rev. Lett. **56**, 2621 (1986).
[7]C. M. Surko and P. Kolodner, Phys. Rev. Lett. **58**, 2055 (1987).
[8]R. Heinrichs, G. Ahlers, and D. S. Cannell, Phys. Rev. A **35**, 2761 (1987); G. Ahlers, D. S. Cannell, and R. Heinrichs, Nucl. Phys. B (Proc. Suppl.) **2**, 77 (1987).
[9]E. Moses, J. Fineberg, and V. Steinberg, Phys. Rev. A **35**, 2757 (1987).
[10]J. Fineberg, E. Moses, and V. Steinberg, Phys. Rev. A **38**, 4939 (1988).
[11]V. Steinberg, J. Fineberg, and E. Moses (to be published).
[12]P. Kolodner, D. Bensimon, and C. M. Surko, Phys. Rev. Lett. **60**, 1723 (1988).
[13]V. Steinberg, G. Ahlers, and D. S. Cannell, Phys. Scr. **32**, 534 (1985).
[14]P. Kolodner, H. L. Williams, and C. Moe, J. Chem. Phys. **88**, 6512 (1988).
[15]W. van Saarlos and P. C. Hohenberg (unpublished).